

Diffusion-Thermo Effects in Stagnation-Point Flow of Air with Injection of Gases of Various Molecular Weights into the Boundary Layer

E M SPARROW,* W J MINKOWYCZ,† AND E R G ECKERT‡

University of Minnesota, Minneapolis, Minn

This paper is concerned with the effect of diffusion thermo on the heat transfer, mass transfer, and flow in a boundary layer into which various foreign gases are injected. Air is the mainstream gas. Particular consideration is given to the question of how the magnitude of the diffusion-thermo effect is related to the molecular weight of the injected gas. Correspondingly, the analysis includes injection of hydrogen, helium, argon, carbon dioxide, and xenon; the selection of these was also influenced by the availability of transport and thermodynamic properties. The study is carried out for plane and axisymmetric stagnation flow in forced convection and for plane stagnation flow in free convection. One effect of diffusion thermo is to create an adiabatic wall temperature T_{aw} different from the stream temperature. It is found that the diffusion-thermo effect is much stronger for injection of H_2 and He (molecular weight less than air) than for injection of A, CO_2 , and Xe (molecular weight greater than air). A heat-transfer coefficient defined with $(T_w - T_{aw})$ as thermal driving force is not strongly affected by diffusion thermo. Additionally, for the case of the highly-cooled wall, the heat-transfer rate is itself not too much affected by diffusion thermo.

Nomenclature

c_p	= specific heat
c_f	= friction coefficient
D_{12}	= binary diffusion coefficient
g	= acceleration of gravity
h	= heat-transfer coefficient
j	= diffusive mass flux
k	= thermal conductivity
M	= molecular weight
Nu	= Nusselt number, hx/k or hr/k
p	= static pressure
q	= heat flux/time area
R	= gas constant
Re	= Reynolds number, $u x/\nu$
r	= cylinder radius
Sc	= Schmidt number, ν/D_{12}
T	= absolute temperature
u	= x component of velocity
u_∞	= freestream velocity
v	= y component of velocity
W_i	= mass fraction, ρ_i/ρ
x	= coordinate along surface
y	= coordinate normal to surface
α	= thermal diffusion factor
μ	= absolute viscosity
ρ	= density
ν	= kinematic viscosity
τ	= wall shear

Subscripts

aw	= adiabatic wall
e	= edge of boundary layer
w	= at the wall
0	= without blowing
1	= injected gas
2	= mainstream gas, air

Introduction

INTEREST in mass-transfer cooling has been stimulated by the need to protect surfaces from high-temperature gas streams such as occur in high-speed flight, rocket exhaust nozzles, and plasma generators. The basic concept of mass-transfer cooling is the release of a relatively cool fluid from the surface into the boundary layer; in this way, there is formed a buffer between the surface and the high-temperature gas stream. There are various specific techniques by which mass-transfer cooling is achieved. The particular processes of interest here involve mass injection that is continuously distributed along the surface.

The initial studies of such mass-transfer cooling processes were concerned primarily with the case in which the mainstream gas and the coolant gas were one in the same, usually air. Later, it was suggested that more effective protection of the surface could be achieved if the molecular weight of the coolant gas were substantially lower than that of the mainstream gas. The use of a "foreign" gas as coolant creates a binary, i.e., a two-component, boundary layer. It was initially believed that the only difference between the single-component and the two-component boundary layer is a variable property effect and a mass diffusion. However, recent wind-tunnel experiments and corresponding analyses for helium injection into air have indicated other effects, namely, thermal diffusion and diffusion thermo. The first of these relates to a diffusive mass flow due to a temperature gradient, whereas the second relates to a heat transfer due to a concentration gradient. Thermal diffusion and diffusion thermo are thermodynamically coupled phenomena. These effects may well be of importance in engineering processes other than mass-transfer cooling, for instance, in evaporation and condensation, rectification, etc.

Pertinent experimental and analytical studies of the helium-air forced-convection boundary layer are summarized in Ref. 1. Of particular significance among these are the analysis of Baron² and the experiments of Tewfik,³ which contain the initial investigations of the diffusional effects as they relate to mass-transfer cooling. Included in Ref. 1 is a detailed analysis aimed at clarifying the effects of thermal diffusion and diffusion thermo on the heat transfer and skin friction in plane and axisymmetric stagnation flow. It was

Received August 26, 1963; revision received February 18, 1964. These studies were supported by a grant from the U S Air Force Office of Scientific Research.

* Professor of Mechanical Engineering, Heat Transfer Laboratory, Department of Mechanical Engineering.

† Instructor of Mechanical Engineering, Heat Transfer Laboratory, Department of Mechanical Engineering.

‡ Professor of Mechanical Engineering, Heat Transfer Laboratory, Department of Mechanical Engineering, Member AIAA.

Table 1 Values of thermal diffusion factor α and Schmidt number Sc for mixtures of various gases with air $T = 590^\circ\text{R}$ (except as noted)

	$W = 0.05$		$W = 0.1$		$W = 0.2$		$W = 0.4$		$W = 0.6$	
	α	Sc	α	Sc	α	Sc	α	Sc	α	Sc
H ₂	-0.292	0.315	-0.339	0.411	-0.398	0.567	-0.457	0.816	-0.510	1.03 ^a
He	-0.324	0.303	-0.371	0.384	-0.448	0.545	-0.594 ^b	1.01 ^b	-0.640	1.22
A	0.0439	0.794	0.0438	0.791	0.0438	0.784	0.0437	0.770	0.0437	0.756
CO ₂	0.0618	0.982	0.0610	0.960	0.0593	0.914	0.0560	0.823	0.0525	0.731
Xe	0.191	1.20	0.189	1.16	0.184	1.08	0.173	0.927	0.152 ^d	0.757 ^d

^a $T = 640^\circ\text{R}$ ^b $W = 0.5$ ^c $W = 0.65$ ^d $T = 540^\circ\text{R}$

shown that, for the adiabatic wall condition, the surface temperature may exceed the freestream temperature by an appreciable amount; this occurs in the absence of aerodynamic heating. These predictions agreed well with experiment. The presence of such an adiabatic wall temperature was demonstrated to be due primarily to diffusion thermo, with thermal diffusion playing a secondary role. For nonadiabatic conditions, when the ratio of wall-to-stream temperature (T_w/T) differs only moderately from unity,[§] it was found that the diffusional effects (especially diffusion thermo) have a decisive effect on heat transfer. Indeed, the heat transfer may be from the fluid to the wall even if $T_w > T$. When T_w/T is much less than unity (highly-cooled wall), the diffusional effects are small.

Corresponding results have been predicted and measured for free-convection flow about a porous horizontal cylinder with helium injection into an air environment. In addition to the diffusional transports, the injection of the foreign gas also was shown to induce a significant buoyancy force above and beyond that induced by temperature differences. This information is summarized in Ref. 4.

In appraising the foregoing results, it is natural to inquire as to whether the effects of thermal diffusion and diffusion thermo are somehow exaggerated for helium injection or whether similar findings apply when other gases are injected into the boundary layer. The exploration of this question is the subject of this paper.

Consideration is given here to binary boundary layers associated with the injection of various gases into a freestream air environment. The transpiring gases were chosen so that the molecular weights of some were smaller than that of air and of others were larger than that of air. It will be seen later that the relative size of the molecular weights of the injected and mainstream gases affects the direction of the mass and energy transports due to thermal diffusion and diffusion thermo. Also a factor in the selection of gases is the availability of reliable thermodynamic and transport properties of the pure substances and of binary mixtures of these with air. Additionally, the diffusional properties of the mixtures are needed. Based on the preceding considerations, the following transpiring gases have been included in this study: hydrogen (2.016), helium[¶] (4.003), argon (39.944), carbon dioxide (44.011), and xenon (131.30). The numbers in parentheses are molecular weights. In this connection, it may be noted that the molecular weight of air is 28.97.

The study to be reported here includes three basic flow configurations: plane and axisymmetric stagnation flows in forced convection, and the plane stagnation flow in free convection. These flows all yield exact solutions of the complete conservation equations; boundary-layer assumptions need not be made. In addition, each one of these flow configurations has already been utilized for experimental studies of helium injection into air. It would be expected that fur-

ther experiments involving other injected gases would utilize these same configurations. In this connection, the free convection configuration appears quite attractive inasmuch as it permits study of the thermal diffusion/diffusion-thermo effect without a wind tunnel.

Thermal Diffusion and Diffusion-Thermo Effects

The diffusive mass flow per unit time and area of species i in a binary gas mixture is related to the concentration and temperature gradients by the equation

$$j_i = -\rho D_{12} \left[\frac{\partial W_i}{\partial y} + \frac{\alpha W_i(1 - W_i)}{T} \frac{\partial T}{\partial y} \right] \quad i = 1, 2 \quad (1)$$

The direction of positive j is in the positive y direction. The local concentration is specified by the mass fraction W ,

$$W_1 = \rho_1/\rho \quad W_2 = \rho_2/\rho \quad \rho = \rho_1 + \rho_2 \quad (2)$$

wherein ρ_1 and ρ_2 are the local densities of species 1 and 2, and ρ is the local density of the mixture. The first term in the brackets of Eq. (1) is the mass diffusion, whereas the second term is the thermal diffusion.

The diffusional properties of the mixture are described by the binary diffusion coefficient D_{12} and the thermal diffusion factor α . In general, the binary diffusion coefficient is positive. However, the sign of α requires more detailed discussion. In particular, if i represents the lighter of the two components, then α is usually negative. Conversely, if i represents the heavier of the two components, then α is usually positive. These signs may be verified by reference to Table 1, which lists α values for mixtures of hydrogen-air, helium-air, and so forth. Taking account of the fore-mentioned sign rule, and using Eq. (2), it is easily verified from Eq. (1) that $j_1 = -j_2$. The sign rule for α may reverse at low temperatures (below room temperature) for some gas mixtures, although such reversals are not encountered for the temperature ranges and gas mixtures involved in this study.

In this investigation, the subscript $i = 1$ will be taken to denote the transpiring gas, while $i = 2$ will denote air. Generally, the highest concentration of the transpiring gas will be at the wall. Therefore, if y is the coordinate normal to the wall, then $\partial W_1/\partial y < 0$, and the mass diffusion gives a positive contribution to j_1 . The thermal diffusion contributes positively to j_1 for light gases (relative to air) when $\partial T/\partial y > 0$ and for heavy gases when $\partial T/\partial y < 0$. On the other hand, the thermal diffusion may oppose the mass diffusion for conditions that are reversed relative to those just stated.

The heat flux per unit time and area in a binary mixture includes both conductive and diffusive contributions

$$q = -k \frac{\partial T}{\partial y} + RT \frac{M^2}{M_1 M_2} \alpha j_1 \quad (3)$$

in which R and M are, respectively, the local gas constant

[§] This is the condition usually found in wind-tunnel experiments.

[¶] Results for helium are taken from Refs. 1 and 4.

and local molecular weight of the mixture, whereas M_1 and M_2 are the molecular weights of the pure components. The first term of (3) is the standard Fourier heat conduction, whereas the second term is the contribution due to diffusion thermo. The sign of α is the same as that used in calculating j_1 in Eq. (1).

Typically, αj_1 will be negative when the transpiring gas is lighter than air. Therefore, the diffusion thermo aids the heat conduction when $\partial T/\partial y > 0$ and opposes the heat conduction when $\partial T/\partial y < 0$. In particular, if Eq. (3) is applied at an adiabatic wall ($q_w = 0$), it follows that $(\partial T/\partial y)_w < 0$. This suggests that the adiabatic wall temperature T_{aw} , corresponding to the injection of a light gas, will exceed the stream temperature T_e .

If the transpiring gas is heavier than air, then αj_1 is typically positive. Therefore, the remarks of the preceding paragraph are reversed. In particular, it appears that $T_{aw} < T_e$ when the transpiring gas is heavy.

Readers interested in the basic physics of the thermal diffusion/diffusion-thermo effect may wish to consult standard works such as Grew and Ibbes,⁵ Chapman and Cowling,⁶ and Hirschfelder, Curtiss, and Bird.⁷

Governing Equations and Their Solution

The flow, heat-transfer, and mass-transfer processes obey the basic principles of momentum, mass, and energy conservation. The mathematical statements of these laws take on somewhat different forms when specialized to the various flow configurations under consideration here. For the plane stagnation flow under forced convection conditions, the appropriate equations are as follows:

$$\rho \left(u \frac{\partial u}{\partial x} + v \frac{\partial u}{\partial y} \right) = - \frac{\partial p}{\partial x} + \frac{\partial}{\partial y} \left(\mu \frac{\partial u}{\partial y} \right) \quad (4)$$

$$\frac{\partial}{\partial x} (\rho u) + \frac{\partial}{\partial y} (\rho v) = 0 \quad (5a)$$

$$\rho \left(u \frac{\partial W_1}{\partial x} + v \frac{\partial W_1}{\partial y} \right) = - \frac{\partial j_1}{\partial y} \quad (5b)$$

$$\rho c_p \left(u \frac{\partial T}{\partial x} + v \frac{\partial T}{\partial y} \right) + (c_{p1} - c_{p2}) j_1 \frac{\partial T}{\partial y} = - \frac{\partial q}{\partial y} \quad (6)$$

The coordinate x measures distances along the surface from the stagnation point, whereas y measures distances normal to the surface.

The first of these represents momentum conservation and has essentially the same form as for a single-component, variable-property flow. Mass conservation is expressed by a continuity equation for the mixture, (5a), and a diffusion equation which conserves species 1, (5b). The diffusive flux j_1 is given by Eq. (1). The energy equation (6) contains two modifications due to the binary nature of the flow. First, there appears on the left side a term representing an additional

convection due to diffusion; second, the heat flux q contains the diffusion-thermo term as represented in Eq. (3).

These same equations may be made to apply to the axisymmetric stagnation flow simply by introducing x as a multiplying factor of ρu and ρv in the continuity equation (5a); for the axisymmetric case, x and y , respectively, correspond to the radial and axial coordinates in a cylindrical system. Equations (4-6) may also be generalized to plane stagnation flow in free convection by replacing the pressure gradient $-\partial p/\partial x$ in Eq. (5) by the buoyancy force.⁴ If such a flow occurs at the lower stagnation point of a horizontal cylinder of radius r , then the appropriate form of buoyancy force is $(g/r)(\rho - \rho_e)x$, in which g is the acceleration of gravity. On the other hand, if the free-convection flow occurs at the upper stagnation point of the horizontal cylinder, then the buoyancy force is $(g/r)(\rho - \rho_e)x$.

The foregoing conservation equations are readily transformed into ordinary differential equations. For each one of the flow configurations, there results from the transformation three** highly coupled, highly nonlinear, ordinary differential equations whose total order is seven. The coupling is due not only to the appearance of the velocity in the energy and diffusion equations, but also to the fact that W and T appear explicitly in the energy and diffusion equations while the fluid properties, which appear in all the equations, depend upon both temperature and concentration. The nonlinearity arises from these same causes. The ordinary differential equations corresponding to the three-flow configurations are stated in Refs. 1 and 4 and need not be repeated here.

Additional coupling between the variables occurs because of the boundary conditions. At the porous surface, it is reasonable to specify the following: $u = 0$ (no slip), $v = v_w$ (specified injection velocity), $v_{a1} = 0$ (surface impermeable to air), $w_1 = w_w$ (specified concentration), $T = T_w$, or $q = 0$ (specified temperature or adiabatic). In the freestream, the following appear reasonable: $u \rightarrow u_\infty$ (specified velocity^{††}), $W_1 \rightarrow 0$ (pure air), and $T \rightarrow T_e$ (specified temperature). The foregoing appear to constitute eight conditions for a set of ordinary differential equations whose total order is seven. However, it can be shown that v_w and W_w cannot be independently prescribed, but rather are coupled through the boundary condition $v_{a1} = 0$.

A necessary prelude to the solution of the governing equations is a knowledge of the thermodynamic, transport, and diffusion properties of the pure gases and of the mixtures of these with air. A description of the methods and equations used in the property computations is presented in the Appendix. These computations require a knowledge of the so-called force constants that are involved in the Lennard-Jones (6-12) representation of the intermolecular forces. The force constants employed in the present property computations are listed in Table 2. It may be noted here that the computation of some of the mixture properties, especially the thermal conductivity k and the thermal diffusion factor α , are exceedingly lengthy.

The actual solution of the governing equations is a formidable numerical undertaking. Not only are the governing equations themselves highly complex, but the computation of the properties is lengthy and involved. To facilitate an iterative method of solution, the governing differential equations were recast into integral form as shown in the Appendix of Ref. 1. To insure convergence of the iterative scheme, a weighted average of the input and output functions for a given cycle of the iteration was used as input to the next cycle. The numerical work was performed on a Control Data 1604 electronic computer at the Numerical Analysis Center of the University of Minnesota.

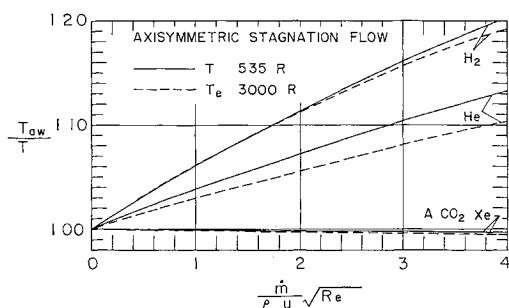


Fig. 1 Adiabatic wall temperature results, axisymmetric forced-convection stagnation flow

** The continuity equation (5a) is eliminated by use of a stream function.

†† For the free-convection case, $u_\infty = 0$.

The cases for which solutions were sought may be subdivided according to the thermal boundary conditions at the wall. The first case is that of the adiabatic wall, whereas the second is that of a prescribed surface temperature. For the latter, solutions were obtained not only for the complete governing equations, but in addition, for modified equations in which the thermal diffusion and diffusion thermo were suppressed. These supplemental solutions were carried out with a view toward correlating the heat-transfer results with and without the diffusional effects.

Results

Adiabatic Wall Temperatures

The existence of an adiabatic wall temperature is due entirely to the action of thermal diffusion and diffusion thermo, particularly the latter. Consequently, the relative magnitudes of the adiabatic wall temperature provide a direct measure of the relative importance of these diffusional effects in various gas mixtures.

The adiabatic wall temperature results are presented in Figs 1, 2, and 3, respectively, for the axisymmetric forced-convection stagnation flow, the plane forced-convection stagnation flow, and the plane free-convection stagnation flow. In each figure, the ratio T_{aw}/T_e is plotted as a function of the blowing parameter (\dot{m} is the rate of mass injection per unit area). For forced-convection stagnation flows, $u \sim x$, and, consequently, the blowing parameter is independent of x . A similar statement applies for the free-convection case. The various curves appearing in each figure are parameterized according to the transpiring gas. In all cases, air is the freestream gas.

The essential aspects of the results are the same for all of the flow configurations; for concreteness, consideration may first be given to the axisymmetric stagnation flow (Fig 1). The solid lines correspond to a freestream temperature of 535°R, which is representative of conditions normally encountered in wind-tunnel experiments on mass-transfer cooling. The dashed curves correspond to 3000°R, which may be somewhat closer to flight conditions.

From an inspection of the figure, it is seen that there is a distinct difference between the results for H_2 and He, which are lighter than air, and those for A, CO_2 , and Xe, which are heavier than air. First of all, the adiabatic wall temperatures for the lighter gases are higher than the stream temperature, whereas the contrary is true for the heavier gases. This finding is in accord with the qualitative discussion of the diffusion-thermo effect which follows Eq (3). That it is diffusion thermo rather than thermal diffusion which is primarily responsible for the adiabatic wall temperature has been quantitatively demonstrated in Refs 1 and 4.

From further observation of Fig 1, one sees that the diffusion-thermo effect is strongly manifested when the transpiring gases are much lighter than air. For instance, for a realistic value of the blowing parameter such as 0.3, the adiabatic wall temperature exceeds the stream temperature by 88°R when the latter is 535°R and the transpiring gas is hydrogen. The adiabatic wall temperatures for hydrogen injection exceed those for helium injection. This suggests that there may be an ordering of the results according to the difference (or perhaps the ratio) of the molecular weights of the transpiring and the freestream gases.

The diffusion-thermo effect is seen to be very slight for the heavier gases. That this should be so for argon and carbon dioxide is not too surprising. These gases are about 50% heavier than air and this is a small difference compared with ratios in weight of $\sim \frac{1}{4}$ for helium and air and $\sim \frac{1}{14}$ for hydrogen and air. However, it is somewhat surprising that xenon, which is about $4\frac{1}{2}$ times heavier than air, displays such a slight diffusion-thermo effect (essentially the same as A and CO_2).

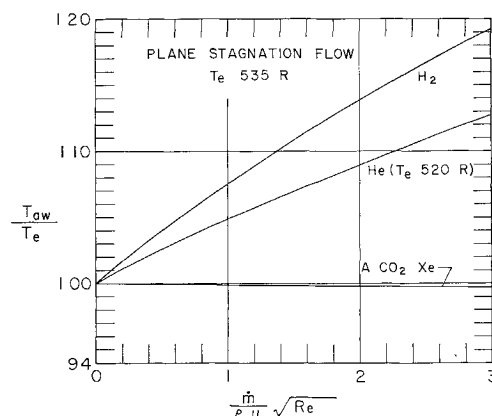


Fig 2 Adiabatic wall temperature results, plane forced-convection stagnation flow

To provide further perspective for these results, it may be interesting to consider the values of the thermal diffusion factor α for various mixtures of hydrogen-air, helium-air, and so forth as listed in Table 1. In considering the table, it is important to realize that information on the thermal diffusion factor is currently in a very elementary state; however, the entries in the table were all computed in a consistent manner and are believed to be as good as any now available. If the thermal diffusion factor were the sole determinant of the adiabatic wall temperature, then the results would be quite different from those of Figs 1-3. In particular, the hydrogen and helium curves would exchange relative positions, and the xenon curve would separate from those of argon and carbon dioxide.

From a study of the governing equations of the problem, one finds that α not only enters alone, but also in a group which includes quantities such as the local mixture molecular weight, local Schmidt number, local gas constant, pure-gas molecular weights, and so forth. The variation of these quantities across the boundary layer is quite different for different gas mixtures, as evidenced by the Schmidt numbers in Table 1. Furthermore, property ratios such as k/k_e , μ/μ_e , ρ/ρ_e , c_p/c_{pe} enter the governing equations. The variation of these across the boundary layer may vary from gas mixture to gas mixture. It is this complex and nonlinear influence of the fluid properties which appears to preclude the formulation of a foolproof rule of thumb for predicting when the diffusion-thermo effect will be large or small.

It is also seen from the figures that the adiabatic wall temperature increases with blowing rate. This is because the diffusion-thermo effect is strengthened with increased blowing ($-\partial W_1/\partial y$ is increased and this increases j_1), and, correspondingly, a higher wall temperature is needed to enable the heat conduction to balance out the q to zero [Eq (3)].

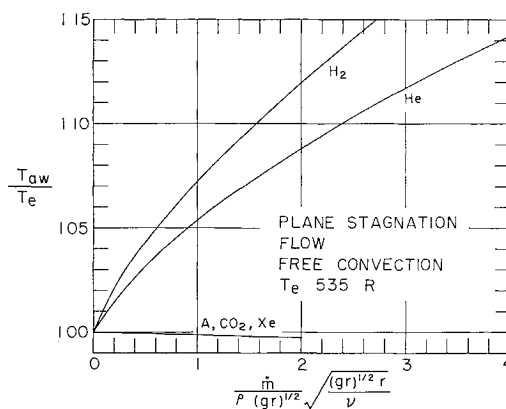


Fig 3 Adiabatic wall temperature results, plane free-convection stagnation flow

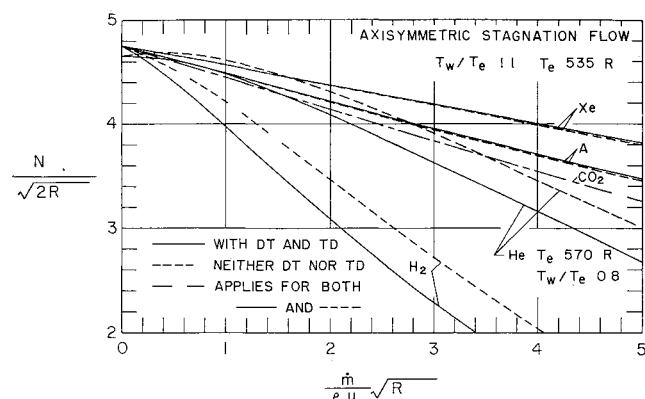


Fig 4a Nusselt number results; axisymmetric forced-convection stagnation flow, $T_w/T_e = 1.1$, $T_e = 535^\circ\text{R}$

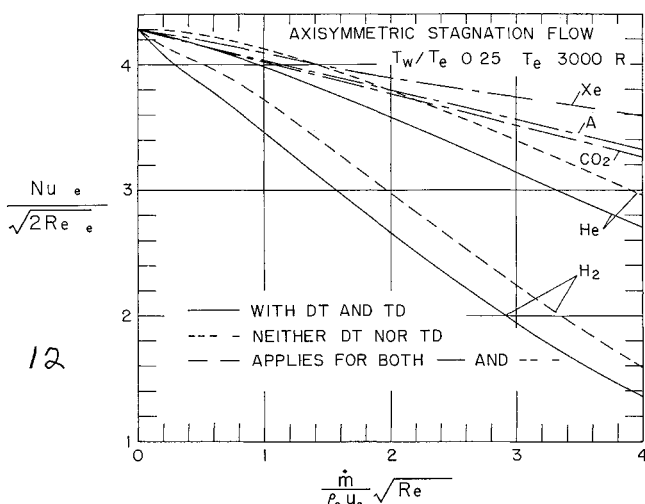


Fig 4b Nusselt number results; axisymmetric forced-convection stagnation flow, $T_w/T_e = 0.25$, $T_e = 3000^\circ\text{R}$

Figure 1 contains results corresponding to T_e values of 535 and 3000°R. The T_{aw}/T_e values for the latter case lie somewhat lower than those for the former. The computations of Ref. 1 for helium-air were carried out for T_e as high as 5000°R, and the forementioned trend continued to be in evidence. Generally speaking, adiabatic wall temperature effects are much more important under laboratory conditions ($T_e \sim$ room temperature) than under flight conditions (large T_e). This can be demonstrated as follows: the heat transfer q_w per unit time and area at the wall may be computed from

$$q_w = h(T_w - T_{aw}) = hT_e [(T_w/T_e) - (T_{aw}/T_e)]$$

For flight applications, the wall generally will be highly cooled, so that $T_w/T_e \ll 1$. Consequently, the heat-transfer rate is not too much affected by the fact that T_{aw}/T_e departs from unity by, say, 10%. On the other hand, for laboratory conditions, T_w/T_e differs only moderately from unity. Since T_w/T_e and T_{aw}/T_e have nearly equal magnitudes, it is clear that q_w is strongly affected by the adiabatic wall temperature. Indeed, even if $T_w > T_e$, the heat will flow from the fluid to the wall if $(T_w/T_e) < (T_{aw}/T_e)$.

In view of the foregoing considerations, calculations for the other flow configurations were confined to the stream temperature $T_e = 535^\circ\text{R}$. The adiabatic wall temperature results for the plane stagnation flow in forced and in free convection are presented in Figs. 2 and 3. Not only are the trends for these configurations the same as those already highlighted for Fig. 1, but also the actual magnitudes of T_{aw}/T_e are very similar for the three configurations. In

connection with the free-convection case, it may be noted that the adiabatic wall results for H_2 and He correspond to the lower stagnation region of the cylinder, whereas those for A , CO_2 , and Xe correspond to the upper stagnation region. This is because a light gas tends to rise in a gravity field and a heavy gas tends to fall in a gravity field.

Heat Transfer and Nusselt Numbers

The surface heat transfer corresponding to prescribed thermal boundary conditions and mass injection rates has been calculated for various transpiring gases. A dimensionless representation of this information can be achieved in terms of the heat-transfer coefficient h and the Nusselt number Nu . A logical definition for h , which takes account of the adiabatic wall temperature, is based on $(T_w - T_{aw})$ as thermal driving force

$$q_w = h(T_w - T_{aw}) \quad (7)$$

in which q_w represents the wall heat flux including both conductive and diffusional contributions [Eq. (3)]. Such a definition has long been standard in situations involving aerodynamic heating and has recently been adapted in the presentation of experimental and analytical results for the transpiration-cooled helium-air boundary layer.

The dimensionless representation of the results for the forced-convection stagnation-flow configurations falls naturally into the grouping

$$Nu_x / (Re_x)^{1/2} \quad (8)$$

wherein $Nu_x = hx/k$ and $Re_x = ux/\nu$. It is easily verified that the foregoing grouping is independent of x ($u \sim x$). For free-convection flow in the stagnation region of a horizontal cylinder of radius r , an appropriate heat-transfer grouping is

$$Nu / [(gr)^{1/2} r / \nu]^{1/2} \quad (9)$$

wherein $Nu = hr/k$.

As was previously mentioned, a set of heat-transfer solutions was also obtained in which the thermal diffusion/diffusion-thermo effects were suppressed. These results also can be represented in terms of the dimensionless groupings of Eqs. (8) and (9), but now h is given by

$$q_w = h(T_w - T) \quad (10)$$

The motivation for considering these auxiliary results is to establish their relationship to the heat-transfer results in which the diffusional effects are included. Of particular interest is the comparison of the heat-transfer coefficients calculated with and without thermal diffusion/diffusion-thermo. If these coefficients are found to have nearly equal values, then it will have been established that the use of $(T_w - T_{aw})$ as thermal driving force essentially removes the diffusional effects from the problem.

A presentation of the heat-transfer results is made in Figs. 4a, 4b, 5, and 6. The first two of these correspond to forced-convection axisymmetric stagnation flow; the last two are for the plane stagnation flow, with Fig. 5 for the forced-convection case and Fig. 6 for the free-convection case. On each figure, the dimensionless heat-transfer grouping is plotted as a function of the blowing parameter, the curves being parameterized according to the transpiring gas. The solid lines correspond to solutions in which thermal diffusion and diffusion thermo are fully accounted for, and the dashed lines correspond to solutions in which these diffusion effects have been suppressed. In those instances where the solid and dashed lines fall on top of one another, a dot-dashed line is employed. The majority of the results correspond to temperature levels appropriate to wind-tunnel and laboratory experiments, that is, $T_e = 535^\circ\text{R}$ and $T_w/T_e = 1.05$ and 1.1. As has been noted, it is for thermal boundary conditions of

this sort that the thermal diffusion/diffusion-thermo effect is strongest. Results for a situation corresponding somewhat more closely to flight conditions ($T = 3000^\circ\text{R}$, $T_w/T = 0.25$) are presented in Fig. 4b for the axisymmetric case.

Consideration may first be given to the forced-convection results for laboratory temperature levels, Figs. 4a and 5. The helium-air results, taken from Ref. 1, do not correspond to precisely the same thermal boundary conditions as do those for the other gases. However, since the temperature variations across the boundary layer are relatively small in all of these cases (~ 50 – 100°F), it is not expected that the forementioned differences in boundary conditions would have an important effect on the results. For concreteness, the discussion will be centered on Fig. 5, on which all the results correspond to $T_w/T = 1.1$.

Upon inspection of the figure, it is seen that, as expected, the Nusselt number generally decreases with increasing blowing. The only exception to this trend is a slight rise in the helium curve at very low blowing rates, and this is due to helium's high thermal conductivity overriding the blowing effect. Further inspection reveals that the Nusselt numbers corresponding to injection of the heavier gases, argon, carbon dioxide, and xenon, are essentially the same with or without the diffusional effects. This is consistent with the findings of Figs. 1–3. Also, since $(T_w - T_{aw})$ is positive and varies very little over the entire range of the blowing parameter for the heavier gases, it follows that the heat transfer q_w is always positive (from wall to fluid) and decreases monotonically with blowing. Furthermore, for these gases, the relative positions of the curves are an index of the relative heat-transfer rates. Thus, the heat transfer is highest with xenon, less with argon, and still less with carbon dioxide. It is interesting to note that these are not strictly ordered according to molecular weight.

The findings for the lighter gases, hydrogen and helium, differ from those just noted. First of all, the Nusselt numbers, i.e., the heat-transfer coefficients, are somewhat different depending upon whether or not the diffusional effects are accounted for. The extent of these deviations vary with the blowing rate, but generally, they are on the order of 5% for helium-air and 10–15% for hydrogen-air. However, these differences are quite small when viewed relative to the differences in the actual heat-transfer rates that are computed with and without the diffusional effects. In particular, for the case in which thermal diffusion/diffusion thermo are suppressed, q_w is always positive for the conditions of Fig. 5. On the other hand, when the diffusional effects are included, q_w decreases rapidly with increasing blowing rate and takes on a negative sign for those blowing rates at which $(T_{aw}/T_e) > (T_w/T)$.

The fact that the hydrogen curves lie below those for helium may be thought to suggest that the former is a more advantageous coolant gas. However, care must be exercised in such judgments, since it is the product of h times $(T_w - T_{aw})$ which is significant and not h alone. It can be verified that the q_w values for hydrogen injection do indeed fall below those for helium injection in the algebraic sense. Thus, at higher blowing rates, when the q_w values for both gases are negative, then those for hydrogen are more negative. For the reasons just discussed, the heat-transfer rates for injection of xenon, argon, and carbon dioxide exceed those for helium, even though the Nusselt numbers for helium lie higher in the range of small blowing rates.

The Nusselt number results for the axisymmetric stagnation flow at laboratory temperature levels (Fig. 4a) exhibit trends that are similar to those already discussed for the plane stagnation case. The only differences are those of numerical detail.

Consideration now may be directed to the results for the axisymmetric stagnation flow under conditions of a relatively high-temperature environment and a highly cooled wall.

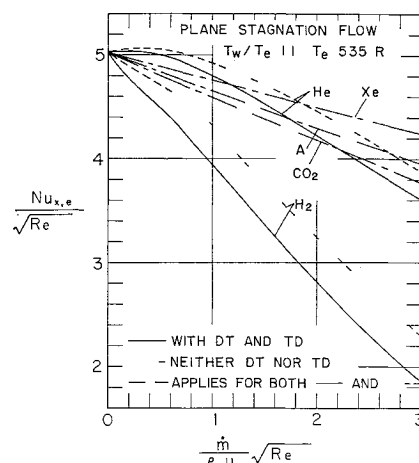


Fig. 5 Nusselt number results, plane forced-convection stagnation flow

(Fig. 4b). As far as general trends are concerned, the results appear to be little different from those of the prior figures. It is, however, worthwhile to point out some further implications. First of all, since $(T_w/T) < (T_{aw}/T)$ for all of the situations dealt with in Fig. 4b, it follows that the heat transfer is from the fluid into the wall in all cases. There is no crossover from positive to negative q_w as in the low-temperature case. Second, although the solid lines for helium and hydrogen injection lie lower than the corresponding dashed lines, the computed heat transfer (to the wall) is slightly greater when the diffusional effects are accounted for than when they are suppressed. Finally, it may be verified that the heat-transfer rates with hydrogen injection are lower than with helium injection.

The free-convection heat-transfer results are presented in Fig. 6. It is seen from the figure that there is a distinctly different behavior depending upon whether the injected gas is heavier or lighter than air. The phenomenon responsible for this is the buoyancy force. When there is no blowing and $T_w > T_e$, the fluid adjacent to the surface is less dense than the mainstream fluid. Consequently, there is a buoyancy-driven upflow about the horizontal cylinder, and the plane stagnation flow solutions apply at the lower stagnation point of the cylinder. If a light gas such as helium or hydrogen is injected into the boundary layer, the temperature-induced buoyancy forces are augmented, and the heat-transfer rates are increased. This accounts for the increase of Nusselt number with blowing rate as evidenced by the upper curves of Fig. 6. At larger blowing rates, the thickening of the boundary layer tends to counteract the buoyancy, and the heat transfer decreases.

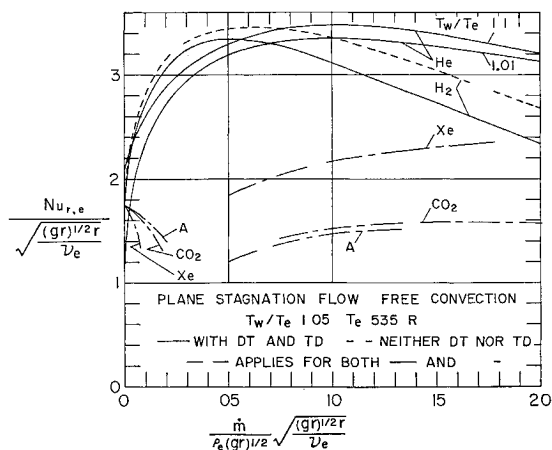


Fig. 6 Nusselt number results, plane free-convection stagnation flow

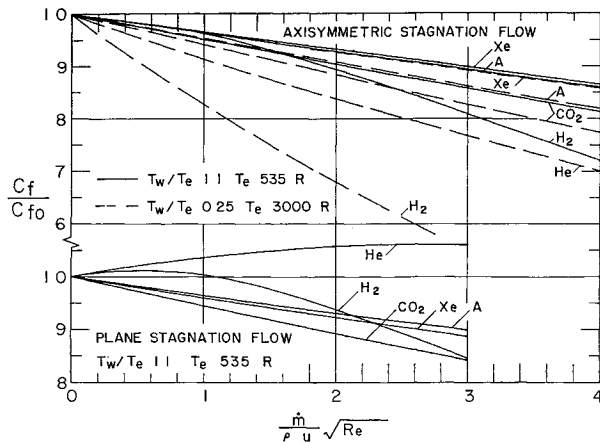


Fig 7 Friction factor results for forced-convection stagnation flows

On the other hand, the effect of a transpiring gas, which is heavier than air, is to oppose the temperature-induced buoyancy and diminish the heat transfer. This is in evidence in the down-sloping curves at the lower left of the figure. For sufficiently high blowing rates, the transpiration-induced buoyancy overrides the temperature-induced buoyancy. Correspondingly, the free-convection flow is downward, and the plane stagnation flow solutions apply at the upper stagnation point. The right-hand segments of the curves for xenon, carbon dioxide, and argon correspond to this situation. Between the two segments is a region where stable solutions could not be found.

Another interesting aspect of the free-convection results is the effect of temperature ratio T_w/T_e . To illustrate this, curves for helium injection are presented in Fig 6 for two temperature ratios, $T_w/T_e = 1.01$ and 1.1 . At very small values of blowing rate, there is a significant difference between the Nusselt numbers for these cases. However, at moderate and higher blowing rates, when transpiration-induced buoyancy overrides the temperature-induced buoyancy, there is little difference in the Nusselt numbers. The effects of thermal diffusion and diffusion thermo are essentially the same as has been discussed in connection with Fig 5.

Skin Friction Results

The shear stress τ exerted by the flowing fluid on the wall may be expressed in dimensionless form by utilizing a friction coefficient c_f defined as follows:

$$c_f = \tau / \frac{1}{2} \rho_e u_e^2 \quad (11)$$

It is convenient to present the effect of blowing on the shear stress in terms of a ratio c_f/c_{f0} , wherein c_{f0} is the friction factor in the absence of blowing. This information is exhibited in Fig 7. The upper part of the figure corresponds to axisymmetric stagnation flow, whereas the lower part of the figure is for plane stagnation flow. Shear stress results for the free-convection flow have little practical utility and are, consequently, not presented here.

As far as this investigation is concerned, the friction results are of secondary interest relative to the thermal results and, therefore, will be discussed only in a general way. There are two basic mechanisms by which blowing affects the skin friction. The first of these is the so-called blow-off effect, whereby the injected mass thickens the boundary layer and reduces the velocity gradients. For a given value of the blowing parameter (abscissa variable of Fig 7), the blowing velocity v_w will be larger when the transpiring gas is lighter. Consequently, one would expect that greater reductions in c_f would be achieved when the transpiring gas is light.

The second effect is related to the fact that a stagnation flow is characterized by an accelerating pressure gradient. In particular, the pressure gradient is imposed by the free-stream flow upon the boundary layer. Such pressure gradients are much stronger in the plane case than in the axisymmetric case. If the density of the fluid in the boundary layer is relatively low compared with that of the freestream fluid (injection of light gas and/or $T_w/T_e > 1$), then the acceleration of the boundary layer is enhanced and a higher skin friction results. On the other hand, if the fluid in the boundary layer is heavier than the freestream flow (injection of a heavy gas and/or $T_w/T_e < 1$), the acceleration of the boundary layer is diminished and a lower skin friction results.

By applying the aforementioned ideas, the trends exhibited in Fig 7 can be explained. The friction factor results are nearly unaffected by the thermal diffusion/diffusion-thermo effect. To complete the presentation, it may be noted that the values of $c_{f0}(Re_e)^{1/2}$ are 2.694 and 2.101 for the axisymmetric case with respective boundary conditions $T_e = 535^\circ R$, $T_w/T_e = 1.1$, and $T_e = 3000^\circ R$, $T_w/T_e = 0.25$. The corresponding value for the plane case with boundary condition $T_e = 535^\circ R$, $T_w/T_e = 1.1$ is 2.550.

Concentration of Transpiring Gas at Surface

It is of some interest to know the relationship between the concentration of the transpiring gas at the surface and the blowing parameter. This information is presented in Fig 8 in terms of the mass fraction W_w , the subscript w denoting wall conditions. The upper part of the figure corresponds to the axisymmetric stagnation flow, whereas the lower part is for the plane stagnation flow. In general, the surface concentration of the transpiring gas increases with the blowing parameter. However, there are certain interesting differences in detail between the trends for the light and the heavy gases. For the light gases, the mass fraction increases relatively slowly for small injection rates and then more rapidly at higher injection rates. For the heavy gases, the opposite trend is in evidence.

Appendix: Computation of Fluid Properties

The thermal conductivity and viscosity of each of the pure (i.e., unmixed) gases were evaluated from expressions based on the Lennard-Jones model for the intermolecular forces. Such expressions may be found in Ref 8, wherein Eq (2i) applies for the thermal conductivity and Eq (3e) for the

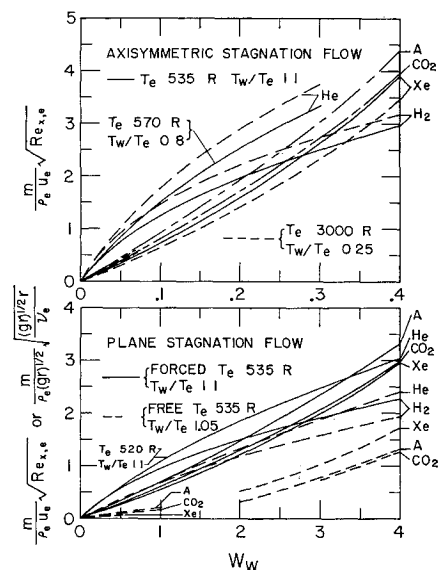


Fig 8 Relationship between wall mass fraction and blowing parameter

Table 2 Force constants for various gases

	Viscosity		Conductivity	
	ϵ/k	σ	ϵ/k	σ
H ₂	38	2 915	38	2 915
He	10 22	2 576	10 22	2 576
Air	84	3 689	154	3 421
A	119 5	3 421	119 5	3 421
CO ₂	213	3 897	309	3 721
Xe	229	4 055	229	4 055

viscosity The force constants required in the evaluation are listed in Table 2 Of these, the numerical values for H₂, He, and Xe are from Ref 7, for CO₂ and air from Ref 9, and for A from Ref 10 In lieu of the foregoing, the thermal conductivity of argon was computed according to an expression on p 11 of Ref 10; however, the argon force constants were utilized in the computation of α

Information on the specific heats of the pure gases was taken from the tabulations of Ref 10, to which curves were fitted In particular, the specific heats of argon and xenon are constant over the temperature range of this study The density was evaluated according to the perfect gas law

For the gas mixtures, the thermal conductivity and viscosity were, respectively, computed by applying Eqs (1) and (3) of Ref 8, whereas specific heat and density were evaluated in accordance with the Gibbs-Dalton mixing rules The computation of the coefficient of mass diffusion D_{12} and of the thermal diffusion factor α was carried out by utilizing Eqs (8 2-44) and (8 2-50) of Ref 7 respectively The collision integrals (i.e., omega integrals) needed in these property calculations were taken from Table I-M of the foregoing reference and were fitted by polynomials for computational convenience

References

- ¹ Sparrow, E M, Minkowycz, W J, Eckert, E R G, and Ibele, W E, "The effect of diffusion thermo and thermal diffusion for helium injection into plane and axisymmetric stagnation flow of air," American Society of Mechanical Engineers Paper 63-HT-23; also J Heat Transfer (to be published)
- ² Baron, J R, "Thermodynamic coupling in boundary layers," ARS J **32**, 1053-1059 (1962)
- ³ Tewfik, O E, Eckert, E R G, and Shirliffe, C J, "Thermal diffusion effects on energy transfer in a turbulent boundary layer with helium injection," *Proceedings of the 1962 Heat Transfer and Fluid Mechanics Institute* (Stanford University Press, Stanford, Calif, 1962), pp 42-61
- ⁴ Sparrow, E M, Minkowycz, W J, and Eckert, E R G, "Transpiration-induced buoyancy and thermal diffusion-diffusion thermo in a helium-air, free-convection boundary layer," American Society of Mechanical Engineers Paper 63-WA-50; also J Heat Transfer (to be published)
- ⁵ Grew, K E and Ibbs, T L, *Thermal Diffusion in Gases* (Cambridge University Press, Cambridge, England, 1952)
- ⁶ Chapman S and Cowling, T G, *The Mathematical Theory of Non-Uniform Gases* (Cambridge University Press, Cambridge, England, 1952)
- ⁷ Hirschfelder, J O, Curtiss, C F, and Bird, R B, *Molecular Theory of Gases and Liquids* (John Wiley and Sons, Inc, New York, 1954)
- ⁸ Eckert, E R G, Ibele, W E, and Irvine, T F, Jr, "Prandtl number, thermal conductivity, and viscosity of air-helium mixtures," NASA TN D-533 (1960)
- ⁹ Novotny J L and Irvine, T F, Jr, "Thermal conductivity and Prandtl number of carbon dioxide and carbon dioxide-air mixtures at one atmosphere," J Heat Transfer **C83**, 125-132 (1961)
- ¹⁰ Hilsenrath, J, Beckett, C W, Benedict, W S, Fano, L, Hoge, H J, Masi, J F, Nuttall R L, Touloukian, Y S, and Wooley, H W, *Tables of Thermodynamic and Transport Properties* (Pergamon Press, Inc, New York, 1960)